Storm Mode and Tornado Potential Determination Using Statistical Moments of Updraft Helicity Distribution

David E. Jahn[1,2], Israel L. Jirak[2], Andrew Wade[1,2], and Jeff Milne[1,2,3]

[1]Cooperative Institute for Severe and High-Impact Weather Research and Operations/Univ. of Oklahoma
[2]Storm Prediction Center/National Weather Service
[3]School of Meteorology/University of Oklahoma

1. Introduction

Updraft helicity (UH) represents the colocation of vertical vorticity and storm updraft and, as such, has been used by various studies as a proxy for identifying right-moving, rotating storms (Thompson et al. 2017, Clark et al. 2013). UH with magnitude exceeding 99.985% of UH climatology for a given convective-allowing model (CAM) has been used to filter right-moving rotating storms as a necessary (albeit not sufficient) condition for forecasting tornadic storms (Gallo et al. 2018, Jahn et al. 2020). Beyond using UH magnitude at a single point, this study analyzes the statistical moments (mean, standard deviation, skewness, kurtosis) of the UH distribution for a storm complex (within a 40-km radius of the point of maximum UH) as a calibration agent for forecasting tornado potential. These UH statistical moments can also be used as means of differentiating storm mode as either a supercell or a mesoscale convective system (MCS).

2. Methodology for Calculating UH Statistical Moments

Using hourly forecast data from individual HREF members initialized at 12Z and valid over a 24-hour period, grid points are identified with UH greater than 99.985% of UH climatology for the given HREF member. A distribution of UH values within a 40-km neighborhood is generated for each filtered grid point. Statistical moments (Table 1) are calculated if the 40-km neighborhood has at least 20 points with UH greater than 25 m^2 s^{-2}. Statistical moments are generated separately at each filtered grid point for each forecast hour and each HREF member. Forecast reflectivity and UH fields are shown for example supercell and MCS cases in Fig. 1. Figure 2 gives UH distributions of the associated supercell and MCS for neighborhood regions coincident with the black circles in Fig. 1. Table 2 gives the calculated statistical moments for these UH distributions. Although the mean of the distributions for both are the same, the distribution shapes for this supercell and MCS cases differ as reflected in skewness and kurtosis values. Trends of these statistical moments, and in particular skewness, are investigated in this study across a relatively large set of cases as a means of differentiating storm mode.

Table 1. Statistical Moments

Mean	$\mu = \frac{1}{n}\left(\sum_{i=0}^{n} x_i\right)$
Standard Deviation	$\sigma = \left[\frac{1}{n}\sum_{i=0}^{n}(x_i-\mu)^2\right]^{1/2}$
Skewness	$= \frac{1}{n}\frac{\sum_{i=0}^{n}(x_i-\mu)^3}{\sigma^3}$
Kurtosis	$= \frac{1}{n}\frac{\sum_{i=0}^{n}(x_i-\mu)^4}{\sigma^4}$

3. Objective I: UH as calibration agent

To investigate UH as a calibration agent, the percentage of observed tornadoes within a 40-km neighborhood are plotted against binned values of specific statistical moments. Figure 3 shows aggregated results from HREF data over a set of over 250 cases occurring April-June of years 2018-2020. There is a general increase in tornado frequency with forecast value of each statistical moment; however, the predicted tornado probability in any case does not exceed 6%, which translates

* *Corresponding author address:* David E. Jahn, CIWRO/Univ. of OK, 120 David L. Boren Blvd., Norman, OK 73072; e-mail: djahn@ou.edu.

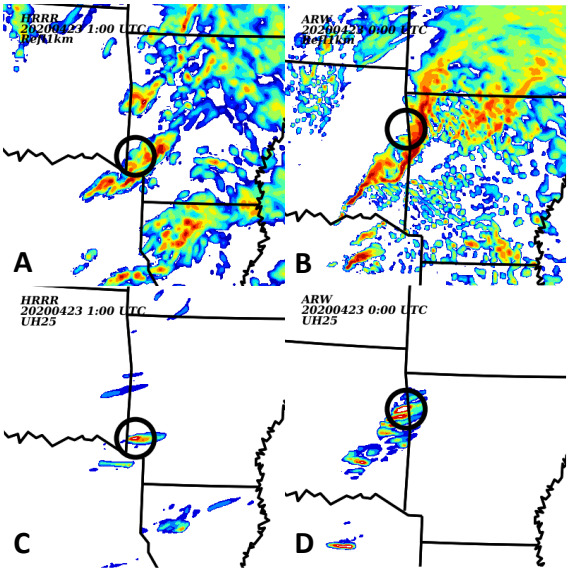

Figure 1. HRRR 13-hour forecast valid at 1 UTC on 4/23/2022 showing A) instantaneous reflectivity, and C) maximum UH [m^2 s^{-2}] for the preceding hour vertically integrated over 2-5 km. Same for subplots B) and D) for ARW 12-hour forecast valid at 0 UTC on the same date. Black circles indicate 40-km neighborhood for defining the UH distribution.

to a low-end slight risk event as defined by the range of tornado outlook severity used by the Storm Prediction Center (SPC) of the National Weather Service (Table 3). These results show that UH statistical moments alone are not sufficient to serve as calibrated agents for determining tornado probability.

4. Objective II: UH distribution to distinguish storm mode

Based on an initial set of cases (not shown but similar to those in Fig. 1), preliminary observations suggest that UH distributions for MCSs generally display a higher number of neighborhood points with lower UH values than higher values. That is, the peak of the UH distribution is offset to the left of the plot (Fig. 2). The UH distribution of the supercell is generally more flat and symmetrical because there are similar number of points representing both low and high UH values. As such, the skewness and kurtosis values are lower for supercells as for MCSs (Table 2).

To test this hypothesis, that skewness, kurtosis, or other statistical moments of the UH distribution could differentiate storm type, a set of 122 cases is analyzed. The first step requires the

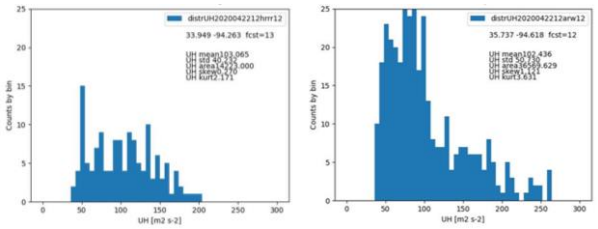

Fig. 2. UH distribution (left) for supercell located at center of circle in Fig. 1 subplots A) and C), and UH distribution (right) for MCS located within circle in Fig. 1 subplots B) and D).

Table 2. Statistical moments for UH distributions of Fig. 2.

Moment	Supercell	MCS
Mean [m2 s-2]	103	102
Std. Dev. [m2 s-2]	40	51
Skewness	0.27	1.12
Kurtosis	2.17	3.63

subjective identification of these 122 cases. An on-line survey is created to allow participants (10 forecasters from the SPC) to identify subjectively storm mode for each case based on plots of forecast reflectivity at 1 km AGL and vertically integrated UH over 2-5 km AGL as generated from HREF data at a time and location of maximum UH within a storm complex (reference circled regions in Fig. 1).

The next step involves mapping by quartiles the distribution of values of the four statistical moments by storm mode based on the 122 cases (74 identified as supercell and 48 as MCS cases). Referencing the 25th to 75th range of values (the boxes in Fig. 4), the mean and standard deviation values are generally higher for supercells than MCSs; however, there is also a relatively large region of overlap that disallows a clear differentiation among these two storm modes. Congruent with what was found for the example cases in Fig. 1, skewness and kurtosis are generally lower for supercells than MCSs and with a smaller overlap in distributions as seen for the mean and standard deviation box plots. The green line drawn for skewness at 1.0 indicates a threshold below which identifies 66% of supercell events, and above which identifies 66% of MCS events. These results give the basis for using a skewness

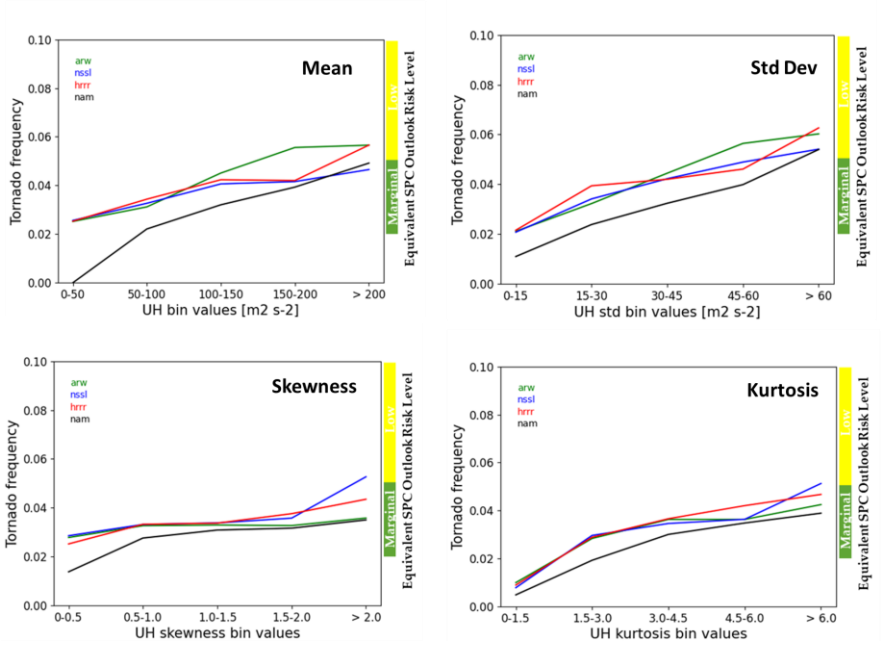

Figure 3. Plots showing the relationship of tornado frequency to bin values of UH statistical moments: mean, standard deviation, skewness, and kurtosis.

Table 3. Range of tornado probability to SPC outlook severity.

Day 1 Outlook Probability	TORN
2%	MRGL
5%	SLGT
10%	ENH
30%	MDT
45%	HIGH

threshold of 1.0 as a means of objectively classifying HREF convective storms as either supercell or MCS.

5. UH-determined storm mode to improve calibrated tornado guidance

Tornado probability related to significant tornado parameter (STP)

Thompson et al. (2017) generated a climatological relationship among STP and tornado frequency (Fig. 5) based on a relatively large set of observed rotating, right-moving discrete storms (i.e., supercells). Here, uniquely for HREF-forecasted MCSs (as identified with skewness greater than 1.0), a relationship is identified among observed tornado frequency and the median of STP that characterizes the inflow region of storm complexes with areas of rotation (e.g., grid points with UH greater than 99.985% of HREF member climatology). Fig. 5 shows significantly lower tornado frequencies for MCSs for the same range of STP values as for supercells, but nonetheless values that are non-zero and increase nearly linearly with higher STP for all HREF members. The exception is the NSSL curve, which exhibits slightly less of an increase in tornado frequency for STP values greater than 2.

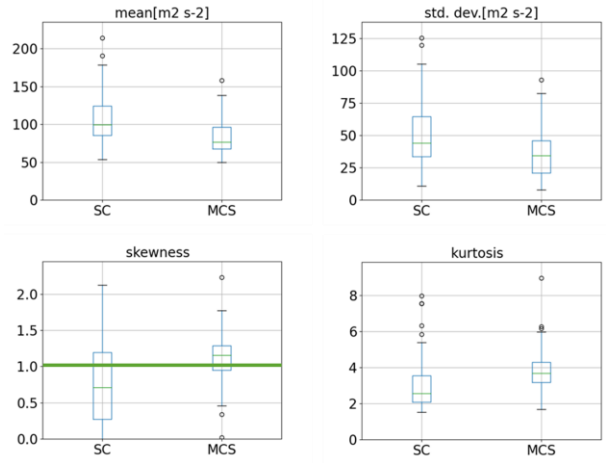

Figure 4. Box and whisker plots showing range of statistical moments grouped by storm mode. Boxes indicate range of 25th to 75th quartiles. The green line drawn at skewness=1.0 described in text.

STP calibrated tornado guidance in consideration of MCS tornado frequency

The supercell tornado frequency (STF) curve and MCS tornado frequency (MTF) curves of Fig. 5 are invoked to calculate tornado potential using an STP calibrated method described in Jahn et al. 2020. In brief, this method uses the median STP value from a distribution of values taken within the inflow region of rotating storms, which are identified within an HREF member forecast at points with a UH threshold greater than 99.985% of UH climatology for the given HREF member. The tornado probability is ascertained at that point

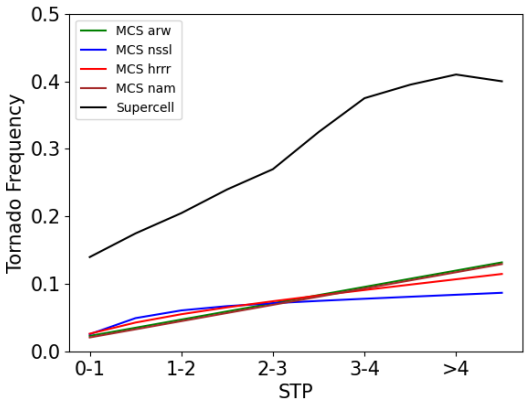

Figure 5. Climatological relationship of STP to tornado probability as described in text. Supercell curve (black) adapted from Thompson et al. 2017. MCS curves given by HREF member according to color in the legend.

based on the median STP and according to the appropriate STF or MTF curve for the storm mode, which is identified as an MCS for skewness greater than 1.0 and supercell less than or equal to 1.0. The final calibrated product reflects the average tornado probability across all HREF members.

Figure 6 shows three cases for which tornado probabilities are calculated using the original calibrated guidance method (such that the STF curve is always invoked regardless of storm mode) and a modified method that uses MTF curves for points with convection classified as an MCS and the STF curve for supercells. The modified method reduces the magnitude and areal coverage of the highest tornado potential contour while generally maintaining the areal footprint of lower (2% and 5%) contour levels. Using 40-km neighborhood

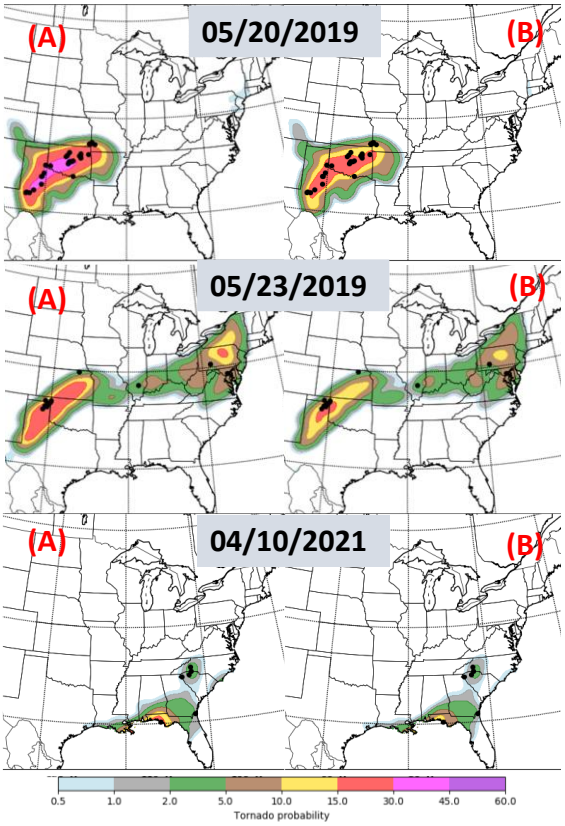

Figure 6. Tornado probabilities for three cases created using an existing STP calibrated tornado guidance method ("A" cases, left column) and using the modified calibration method ("B" cases, right column).

verification, the modified method results in an increase in aggregate CSI for the three cases by 4%, 12.5%, 49%, and 42% respectively for the tornado probability thresholds of 2%, 5%, 10%, and 15%. Referencing the SPC definition of categorical tornado outlook intensity (Table 3), greatest forecast improvement occurs for scenarios exhibiting low- to mid-level enhanced outlook intensity (10-15% tornado probability).

6. Summary

Using HREF data for a set of 250+ cases from the spring periods of 2018-2020, an increase in observed tornado frequency does show some correlation with an increase in each of the four UH distribution statistical moments (mean, standard deviation, skewness, and kurtosis). However, these moments are not sufficient by themselves as a calibration agent for differentiating tornadic storms.

Based on a study of 122 cases, skewness is shown to be a reasonable objective differentiator of storm mode using a threshold of 1.0, above which indicates a higher likelihood of MCSs and below which indicates supercells. Invoking this skewness threshold, it is possible to identify a relationship among STP and tornado frequency strictly for MCS cases based on historical HREF. Very preliminary results show that invoking this MCS tornado frequency curve can improve calibrated tornado guidance especially in the low- to mid-level enhanced range of tornado outlook probabilities (10-15% range). These results are based on three cases and thus highly preliminary. Future work will investigate the effectiveness of the modified calibrated method using a much larger test set.

7. Acknowledgements

Funding provided by NOAA/Office of Oceanic and Atmospheric Research under NOAA-University of Oklahoma Cooperative Agreement #NA21OAR4320204, U.S. Dept. of Commerce. The statements, findings, conclusions, and recommendations are those of the author(s) and do not necessarily reflect the views of NOAA or the U.S. Department of Commerce.

8. References

Clark, A. J., J. Gao, P. T. Marsh, T. Smith, J. S. Kain, J. C. Correia Jr., M. Xue, F. Kong, 2013: Tornado pathlength forecasts from 2010 to 2011 using ensemble updraft helicity. *Wea. Forecasting*, 28, 387-407.

Gallo, B. T., A. J. Clark, B. T. Smith, R. L. Thompson, I. Jirak, 2018: Blended probabilistic tornado forecasts: Combining climatological frequencies with NSSL-WRF ensemble forecasts. *Wea. Forecasting*, 33, 443-459.

Jahn, D. E., B. T. Gallo, C. Broyles, B. T. Smith, I. Jirak, J. Milne, 2020: Refining CAM-based tornado probability forecasts using storm-inflow and storm-attribute information. 26th Conf. on Numerical Weather Pred., Boston, MA, Amer. Meteor. Soc.

Thompson, R. L., B. T. Smith, J. S. Grams, A. R. Dean, J. C. Picca, A. E. Cohen, E. M. Leitman, A. M. Gleason, and P. T. Marsh, 2017: Tornado damage rating probabilities derived from WSR-88D data. *Wea. Forecasting*, 32, 1509-1528.